

DESIGN, GROWTH, FABRICATION AND CHARACTERIZATION OF HIGH-BAND GAP InGaN/GaN SOLAR CELLS

Omkar Jani¹, Christiana Honsberg², Yong Huang¹, June-O Song¹, Ian Ferguson¹, Gon Namkoong¹, Elaissa Trybus¹, Alan Doolittle¹, Sarah Kurtz³

1. School of Electrical and Computer Engineering, Georgia Institute of Technology, Atlanta, GA, USA 30332
2. Department of Electrical and Computer Engineering, University of Delaware, Newark, DE, USA 19716
3. National Renewable Energy Laboratories, Golden, CO, USA 80401

ABSTRACT

One of the key requirements to achieve solar conversion efficiencies greater than 50% is a photovoltaic device with a band gap of 2.4 eV or greater. $\text{In}_x\text{Ga}_{1-x}\text{N}$ is one of a few alloys that can meet this key requirement. InGaN with indium compositions varying from 0 to 40% is grown by both metal-organic, chemical-vapor deposition (MOCVD) and molecular beam epitaxy (MBE), and studied for suitability in photovoltaic applications. Structural characterization is done using X-ray diffraction, while optical properties are measured using photoluminescence and absorption-transmission measurements. These material properties are used to design various configurations of solar cells in PC1D. Solar cells are grown and fabricated using methods derived from the III-N LED and photodetector technologies. The fabricated solar cells have open-circuit voltages around 2.4 V and internal quantum efficiencies as high as 60%. Major loss mechanisms in these devices are identified and methods to further improve efficiencies are discussed.

INTRODUCTION

The goal of achieving photovoltaic conversion efficiencies of 50% or higher not only attributes as a scientific achievement and aids specialized applications, but can also reduce the cost of large-scale solar electric generation. The maximum reported photovoltaic efficiency of 39% at 236 suns is achieved by a triple-junction GaInP-GaInAs-Ge tandem solar cell [1]. While the achievable efficiency of triple-junction tandem solar cells is restricted to about 40% [2], modeling results show that a tandem solar cell of five junctions or greater, or an equivalent structure, is required to achieve practical efficiencies of greater than 50% under an AM1.5 spectrum and a realistic concentration of 500x [1,3]. These structures require band gaps of the top cell to be at least 2.4 eV. InGaN has the appropriate optical properties and has been well demonstrated for light-emitting applications. In this paper, we study the design of InGaN solar cells based on device physics and the unique properties of InGaN. We first discuss the present state of development for this material system and use it to design the preliminary solar cell. We then grow InGaN by MOCVD and characterize it to further

optimize the device design. Test solar cells are grown and tested, and methods to further increase the performance of these devices are discussed.

InGaN MATERIAL SYSTEM

The III-Nitride semiconductor system, which includes AlN, GaN, InN and its alloys provides all band gaps needed to construct solar cells with response above 2.4 eV. The nitrides also have high charge velocities [4] and strong light absorption. InGaN LEDs are relatively insensitive to high dislocation densities and have unusual polarization and piezoelectric properties [5,6]. The III-N material system has undergone remarkable development due to the use of GaN and $\text{In}_x\text{Ga}_{1-x}\text{N}$ for blue LEDs and laser diodes [7]. MOCVD has emerged as the leading candidate for commercial growth of high band gap InGaN due to its large scale manufacturing potential. A major challenge for the MOCVD growth of InGaN is to reduce its band gap and achieve efficient light emission in the blue-green region. This material can be used as the highest band gap material in a solar cell with five-junctions or greater. InN and In-rich low-band gap InGaN are commonly grown by MBE. Recently the band gap of InN was shown to be lower than previously thought [8,9,10]; low band gap InGaN is a subject of fundamental study.

Phase separation of InGaN at high In concentrations

Phase separation is commonly observed in InGaN films with high In compositions due to the low miscibility of InN in GaN. Theoretical calculations [11] based on a valence-force-field (VFF) model [12,13] predict that phase separation in InGaN strongly depends not only on the temperature and In composition, but also on the strain state of the InGaN films. For example, at a growth temperature of 800°C, the predicted maximum In composition allowable before phase separation occurs is less than 6%. However, biaxial strain can suppress In phase separation and acts as a driving force to form ordered structures. In relaxed films, spinodal decomposition occurs below a critical temperature and for a range of alloy compositions that defines miscibility at a given temperature [14]. However, it is known that this critical temperature can be significantly reduced due to

biaxial strain and also the miscibility gap can be suppressed [15]. Therefore, In phase separation can be controlled by managing biaxial strain, using a strained system of InGaN/GaN [14]. It is critical to eliminate phase separation the phase separated material with the lowest band gap dominates the V_{OC} of the solar cell.

P-type doping

Achieving p-type conductivity in InGaN alloys is difficult partly due to a high background concentration of donors that arise from native defects. P-type GaN can be achieved by improving the structural quality of GaN, but is limited to $<10^{18} \text{ cm}^{-3}$ hole concentration due to the deep activation energy of acceptors [16]. Compared with GaN, InGaN has been shown to possess higher background donor concentrations of $\sim 10^{19} \text{ cm}^{-3}$; these donors compensate intentionally added acceptors [17]. For In compositions greater than 32% p-type conductivity over the entire sample has not yet been reported, indicating that growth of p-type InGaN is difficult. However, solar cells using heterostructures can be designed using higher band gap InGaN as the p-type region. This design has the additional advantage that light absorption is enhanced in the field region, with the p-type layer acting somewhat as a window layer.

Piezoelectric polarization and band bending

A unique feature for the III-nitrides is strong polarization and piezoelectric effects [5,6]. These are highly polar molecules, and hence, develop a large dipole at interfaces between the materials inducing an electric field in the bulk region between two surfaces. Piezoelectric fields may also be induced in the material by strain from lattice mismatch. The high piezoelectric coefficients modify the surface potentials and generate electric fields across the materials, and hence are critical in the interpretation of transport properties of the material [18]. This phenomenon tends to enhance transport of carriers potentially moderating the effect of high dislocation densities.

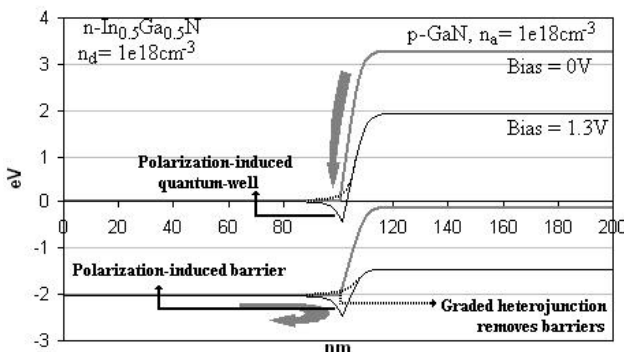


Fig. 1. Simulated band diagram of GaN/In_{0.5}Ga_{0.5}N graded and abrupt heterojunction under forward bias.

A consequence of polarization is the strong band bending at junctions of the III-Nitride materials. This band bending may be used to reduce surface recombination

velocities enhancing the performance of the solar cell. However, band bending at the junctions in heterojunction InGaN solar cells tend to create barriers and wells that restrict minority carriers from diffusing and being collected as shown in Figure 1. This effect, caused by an abrupt heterojunction interface, can be nullified using a graded heterojunction transition as shown in the figure.

Lifetime and diffusion lengths

Diffusion lengths, which in turn relate to the minority carrier lifetimes, are a critical parameter in the solar cell performance. The III-Nitrides demonstrate a very low diffusion length due to high dislocation densities; the best reported lifetimes are around 6.5ns [19,20]. However, the transport of minority carriers is enhanced due to polarization fields within the material. Moreover, as the III-Nitrides have a high absorption coefficient, very thin layers of the material are sufficient to absorb most of the light. Hence, the short diffusion lengths are adequate for photocarrier collection.

Ohmic contact to p-InGaN

One of the major challenges in the III-Nitride technology is to form a low resistance Ohmic contact with p-type material. Due to the high work-function of p-InGaN, no readily available metal can form an Ohmic contact with it. However, recently developed metallurgical junctions have achieved specific contact resistances as low as $10^4 \Omega/\text{cm}^2$ [21]. Through band gap engineering, a short-period superlattice (SPS) structure can be grown that combines the p-type layer with the well material to form an Ohmic contact [22]. This kind of a structure also enhances lateral transport of the carriers improving collection probability.

Substrates

The III-nitrides typically crystallize in a wurtzite crystal structure, unlike Si, Ge, and GaAs which crystallize in a diamond or zinc-blend structure. Sapphire is the most commonly used substrate for the growth of wurtzite GaN. However, due to the large lattice and thermal mismatches between sapphire and III-Nitrides (16% for GaN on sapphire and 29% for InN on sapphire), epitaxial films on sapphire result in dislocation densities typically in the 10^7 - 10^{10} cm^{-2} range. Other substrates are SiC and ZnO which provide better lattice match, but nevertheless have similar dislocation densities. However, the III-Nitrides have an apparent insensitivity to high dislocation densities due to strong polarization within the material. Moreover, sapphire substrates, due to superior mechanical and optical properties, can be used as an encapsulant material for a flip-chip solar cell.

DEVICE DESIGN

GaN LED and photodetector structures are taken as a starting point for design of GaN solar cells. These structures include standard GaN p-i-n diodes, GaN p-i-n with InGaN quantum-wells (QW) and GaN p-i-n with InGaN as the i-region. The structures are modified to optimize light absorption, instead of emission as in LEDs,

and collection without any external bias, contrary to conventional photodetector structures. The p- and n-regions are consistently doped at $5 \times 10^{17} \text{ cm}^{-3}$ and $5 \times 10^{18} \text{ cm}^{-3}$, respectively, to comply with optimized growth settings from previous experiments.

The literature indicates a high absorption coefficient for InGaN ($>10^5 \text{ cm}^{-1}$ at the band edge). As a result, the material absorbs more than 95% of the incident light within the first 300 nm and more than 99% within the first 500 nm. Hence, the total thickness of the device is limited to 500 nm.

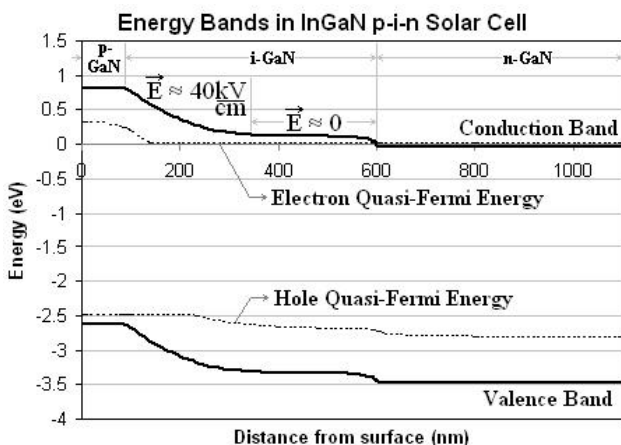


Fig. 2. Energy bands of a GaN p-i-n solar cell calculated in PC1D indicating an effective electric field within the first 200 nm of the i-region.

The solar cells are designed to optimize light absorption in the field-bearing i-region for maximum collection. However, due to a background n-type concentration of 10^{16} cm^{-3} present in i-InGaN, the electric field within this region is maintained only up to a certain distance from the p-GaN interface, after which it effectively becomes zero. PC1D simulations of the device indicate that an effectively uniform electric field is maintained only within the first 200 nm of the i-region as shown in Figure 2. A 200 nm thick i-region yields an average electric field of about 40 kV/cm. Hence, the thickness of the i-GaN layer in the solar cell is limited to 200 nm.

The thickness of the p-region is to be minimized so that most of the light is absorbed by the i-region. However, the p-region should be thick enough to provide enough charge for the depletion region as well as the top metal contact. Samples grown previously by MOCVD measured minority hole and electron diffusion lengths of 0.2 μm and 1.44 μm , respectively, restricting the thickness of the n- and p-regions to these values. Hence, the p-region thickness is chosen as 100nm, while the metal contact at the n-region is determined to be at a distance of 200 nm from the i-region.

These design rules can be applied to similar InGaN p-i-n structures as well as heterojunction devices. The i-GaN layer can be replaced by novel materials like InGaN to test for photovoltaic properties. Difficult to grow

materials can be pseudomorphically grown as quantum wells to form structures similar to quantum-well solar cells.

GROWTH OF InGaN

InGaN with In concentrations ranging from 0 to 40% are grown on a standard 2" sapphire wafer by MOCVD. The in-situ reflective measurement data of a typical InGaN growth process is shown in Figure 3. First, a low temperature GaN nucleation layer is grown on the sapphire substrate to stop the propagation of defects arising from lattice mismatch with sapphire into the InGaN growth on top. Then a 2- μm thick high-quality GaN template is grown, which minimizes the lattice mismatch for the InGaN grown for characterization.

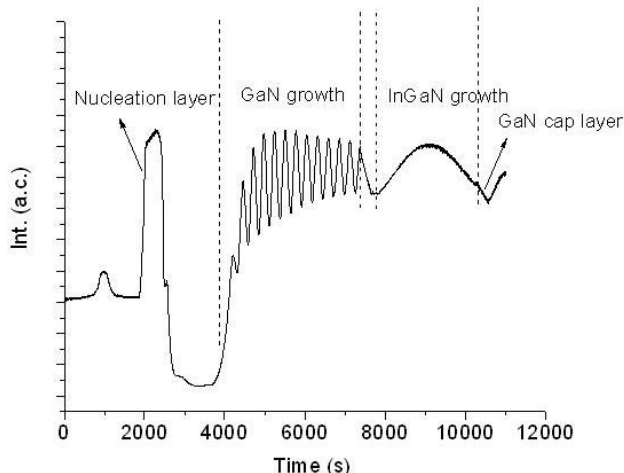


Fig. 3. In-situ reflective measurement data of a typical InGaN growth by MOCVD.

The motivation for these growths is to produce low band gap InGaN that is suitable for use in photovoltaics. Precise control of the composition, thickness, uniformity and doping levels is investigated. The variables optimized during InGaN growth are temperature and gas flows, which primarily govern the growth rate. The structural composition of the grown material is verified with X-ray diffraction (XRD), while its corresponding band gap is verified by its photoluminescence (PL).

Additionally, the solar cells designed earlier are also grown to characterize for material quality as well as device performance. Solar cells are grown on u-GaN buffer layers as well as on a 500-nm thick AlN template. As AlN does not effectively absorb light, this template can be used for back-side illumination devices, where light is incident on the substrate-side of the solar cells.

FABRICATION OF InGaN SOLAR CELLS

Preliminary p-i-n structures similar to those shown in Figure 4 are grown by MOCVD. The i-GaN is replaced by i-In_xGa_{1-x}N with x=0.04, 0.05. Quantum-well solar cells are grown by incorporating 5 quantum wells of 5-nm-wide In_{0.1}Ga_{0.9}N separated by 10-nm-wide GaN barriers in the i-

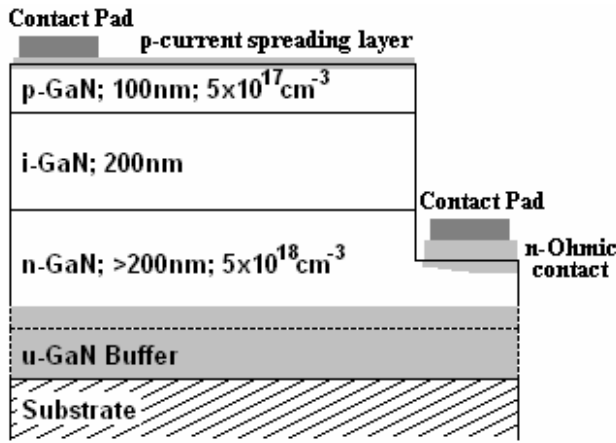


Fig. 4. A fabricated GaN p-i-n solar cell structure.

region. Finally, a p-i-n structure is grown on a 500-nm u-AlN template.

First, an isolation etch to isolate each device and then a mesa etch to expose the n-region for contact is performed using a PlasmaTherm ICP etching tool. Then a 5-nm-Ni/5-nm-Au layer is deposited to form a current-spreading layer on the p-GaN by electron-beam evaporation. An n-Ohmic contact layer is formed by depositing 10-nm-Ti/30-nm-Al/10-nm-Ti/50-nm-Au. Finally, a 50-nm-Ni/50-nm-Au thick deposition is made on the p-current spreading layer for external contacts. As Ni forms a Schottky contact with p-GaN, the p-current spreading layer is annealed in an O_2 ambient to convert the Ni to NiO_x . The n-Ohmic contact is also annealed in a N_2 ambient to form Ti_xN_y and Al_xN_y compounds that reduce contact resistance.

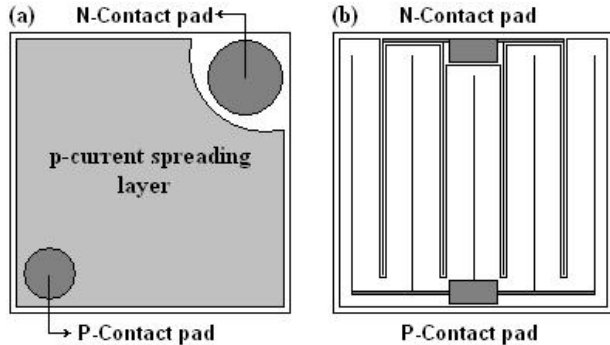


Fig. 5. (a) LED style and (b) grid designs used to contact the solar cells.

Solar cells of sizes ranging from 1 mm x 1 mm to 5 mm x 5 mm are fabricated. Two designs to contact the p-GaN layer are tested as shown in Figure 5. The first design consists of a spread-out p-current spreading layer, which is commonly used for LEDs. However, calculations show that this layer can absorb up to 50% of the incident light. Hence, a second design for contacting p-GaN is used where the p-current spreading layer is deposited in the form of grids.

RESULTS

Growth

$In_xGa_{1-x}N$ with x ranging from 0 to 0.4 is grown primarily to check the suitability of the material for photovoltaic applications. Figure 6 gives the comprehensive XRD patterns of InGaN to verify its In composition and structural quality. A distinct GaN (0002) peak for the template is seen at $\theta = 17.28^\circ$, while the InGaN (0002) peaks give the respective In composition. The XRD shows a good crystalline quality for InGaN with higher In compositions, while a deterioration is observed for In compositions greater than 30%. Additional In (101) peaks are observed indicating a small amount of segregated In droplets.

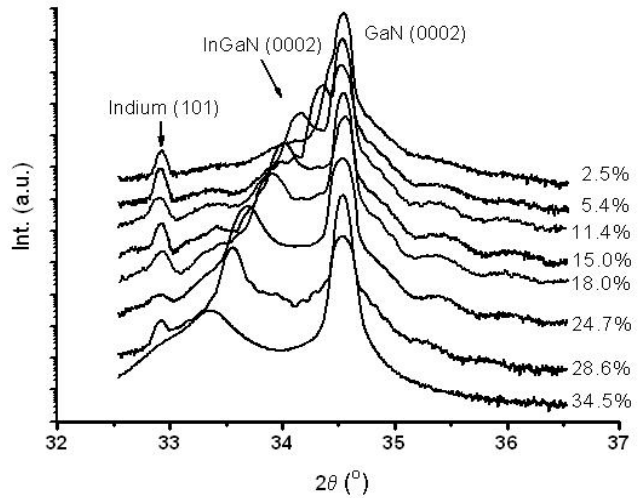


Fig. 6. XRD data for InGaN with variable In compositions grown by MOCVD.

The material is further characterized for optical consistency and phase separation by PL. Figure 7 summarizes the optical band gaps, derived from PL peaks, for various In compositions in InGaN, derived from XRD data. The primary PL peaks indicating the optical band gaps match closely to previously measured band gaps by Nakamura *et al* [23]. However, a few samples show secondary PL peaks indicating the presence of a phase-separated InGaN. The presence of phase separated

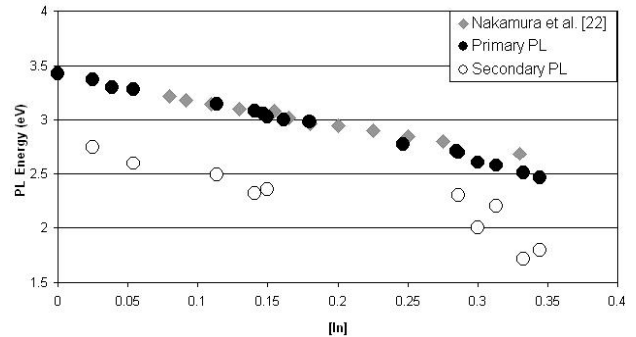


Fig. 7. PL emission energy versus In composition for InGaN grown by MOCVD.

InGaN is more evident at higher In compositions as PL intensity for the secondary phase emission increases for these In compositions.

Material characterization results show that In composition in InGaN is primarily determined by the growth temperature. Increasing the temperature while decreasing the In-carrier gas flow rate suppresses the PL emission from the secondary phase-separated material. Growth rate is enhanced by increasing the Ga-carrier gas flow rate, but deteriorates crystal quality.

Device

The InGaN is further characterized through the device data. Spectrometry measurements of $\text{In}_{0.05}\text{Ga}_{0.95}\text{N}$ in a solar cell confirm its absorption edge at the band gap of 3.26 eV, as shown in Figure 8. The high absorption coefficient of greater than 10^5 cm^{-1} is confirmed for the material.

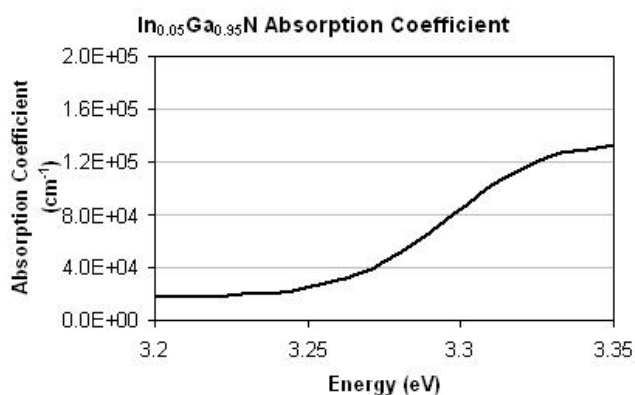


Fig. 8. Absorption coefficient of $\text{In}_{0.05}\text{Ga}_{0.95}\text{N}$ at its band edge.

The p-type current-spreading layer deposited on the front surface of GaN is characterized for absorption and reflection. This layer reflects 20-30% and absorbs up to 50% of the incident light depending on the Ni and Au compositions. The reflection and absorption of this layer decreases after oxidizing by annealing in O_2 .

The illuminated I-V curve for the GaN p-i-n solar cell, with a p-type current-spreading layer similar to that in LEDs, is shown in Figure 9. Even though $\text{In}_{0.05}\text{Ga}_{0.95}\text{N}$ is incorporated as the i-region of the device, phase-separated InGaN with band gap of 2.8 eV dominates the V_{OC} of the device. These solar cells give a V_{OC} of around 2.4 V under UV illumination. Although the devices contacted using a grid pattern give higher V_{OC} 's, they encounter a Schottky barrier at the metal contact, increasing the series resistance and decreasing the overall efficiency of the cell.

The internal quantum efficiency (QE) measurements shown in Figure 10 indicate a QE of 60% at the band edge. The sharp QE edge is consistent with the band gap indicated by XRD, PL and the absorption edge of the material discussed earlier. Absorption of light by the p-type current-spreading metal layer is the major loss

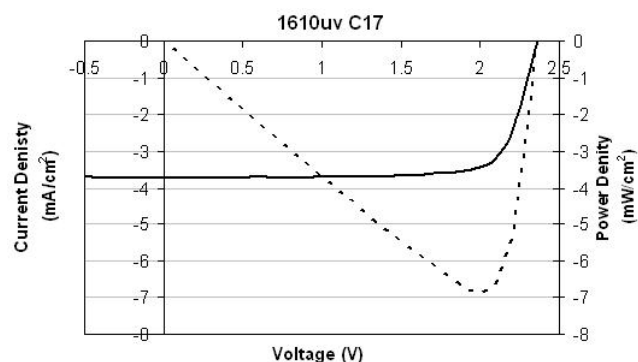


Fig. 9. I-V characteristic of a GaN p-i-n solar cell with $\text{In}_{0.05}\text{Ga}_{0.95}\text{N}$ as the i-region.

mechanism in the QE. Moreover, the heterojunction interfaces act as recombination sites decreasing the photocurrent.

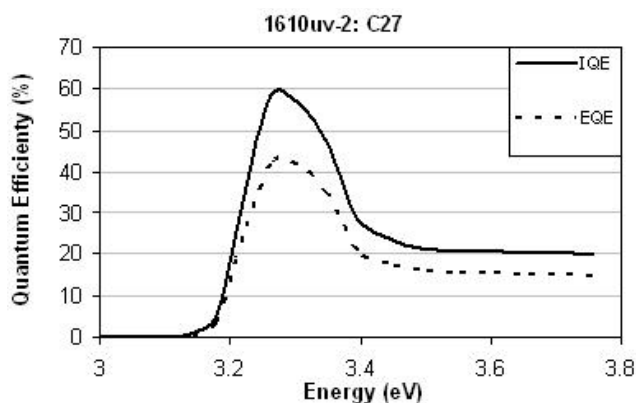


Fig. 10. QE for the GaN p-i-n solar cell with $\text{In}_{0.05}\text{Ga}_{0.95}\text{N}$ as the i-region.

DISCUSSION

Methods to increase the V_{OC} and QE of the GaN and InGaN solar cell are investigated. As the phase-separated material dominates the V_{OC} of the solar cell, growth of InGaN has to be optimized using the observations mentioned earlier.

The intrinsic region of the solar cell contributes to the series resistance to a large extent, which measures up to 30Ω . PC1D simulations show that although removing this intrinsic region decreases the J_{SC} of the cell, it enhances the efficiency by increasing the V_{OC} by a higher order of magnitude. The J_{SC} can be enhanced further by introducing light trapping. Simulations also indicate that removing the GaN/ $\text{In}_{0.05}\text{Ga}_{0.95}\text{N}$ heterojunctions increase the QE of the solar cell by about 15%.

Schottky barriers formed at the p-GaN/Ni interface tend to decrease photocurrent and V_{OC} of the device. Moreover, the p-type current-spreading layer absorbs a significant fraction of the incident light. Hence, the p-GaN contacting scheme is a crucial component in reducing losses for the solar cell. In addition to optimizing the metallurgical junctions formed by annealing, advanced nanostructures like the SPS structures can also be used.

CONCLUSION

Various aspects of the InGaN material for applications in high-efficiency photovoltaics are discussed. A systematic study of the MOCVD growth of InGaN with In compositions varying from 0 to 40% is performed. InGaN, with up to 30% In composition, is shown to demonstrate structural and optical characteristics suitable for photovoltaics. Fabricated GaN/InGaN devices using this material give a consistent V_{OC} of 2.4 V and IQE as high as 60%. Moreover, methods to further increase the performance of these solar cells are investigated and discussed.

ACKNOWLEDGEMENTS

This work was partially funded by DARPA/ARO Agreement No.: W911NF-05-9-0005. This work was also supported by U.S. D.O.E. and the National Renewable Energy Laboratories, monitored by Dr. Robert McConnell and Dr. Martha Symko-Davies, and the Office of Naval Research, monitored by Dr. Colin Wood.

REFERENCES

- [1] R.R. King, D.C. Law, C.M. Fetzer, R.A. Sherif, K.M. Edmondson, S. Kurtz, G.S. Kinsey, H.L. Cotal, D.D. Krut, J.H. Ermer, N.H. Karam, "Pathways to 40% Efficient Concentrator Photovoltaics," Proceedings of the 20th Eu. PVSEC, 2005, pp. 118–123.
- [2] O. Jani, C. Honsberg, A. Asghar, D. Nicol, I. Ferguson, A. Doolittle, S. Kurtz, "Characterization and Analysis of InGaN Photovoltaic Devices," Proceedings of the 31st IEEE PVSC, 2005, pp. 37-42.
- [3] A. Devos, "Endoreversible Thermodynamics of Solar Energy Conversion," OUP, 1990.
- [4] Y. Nanishi, Y. Saito and T. Yamaguchi, "R-F Molecular Beam Epitaxy Growth and Properties of InN and Related Alloys", *Jpn. J. Appl. Phys.*, **42**, 5A, 2003, pp. 2549-2559.
- [5] F. Bernardini, and V. Fiorentini, "Nonlinear Macroscopic Polarization in III-V Nitride Alloys", *Phys. Rev. B*, **64**, 8, 2001, pp. 085207/1-7.
- [6] V. Fiorentini F. Bernardini, "Spontaneous versus Piezoelectric Polarization in III-V Nitrides: Conceptual Aspects and Practical Consequences", *Phys. Stat. Sol. B*, **216**, 1, 1999, pp. 391-398.
- [7] S. Nakamura, S. Pearton, G. Fasol, "The Blue Laser Diode, 2nd Ed.", Springer-Verlag, 2000.
- [8] V. Yu. Davydov et al., "Absorption and Emission of Hexagonal InN. Evidence of Narrow Fundamental Band Gap," *Phys. Stat. Sol. B*, **229**, 3, 2002, pp. R1-R3.
- [9] J. Wu et al., "Temperature Dependence of the Fundamental Band Gap of InN", *J. Appl. Phys.*, **94**, 7, 2003, pp. 4457-4460.
- [10] T. Matsuoka, H. Okamoto, M. Nakao, H. Harima, and E. Kurimoto, "Optical Bandgap Energy of Wurtzite InN", *Appl. Phys. Lett.*, **81**, 7, 2002, pp. 1246-1248.
- [11] V.A. Elyukhin, S.A. Nikishin, "Internal Strain Energy of $A_x^3B_{1-x}^3N$ Ternary Solid Solutions of Cubic Modification," *Semicond. Sci. Technol.*, **11**, 1996, pp. 917-920.
- [12] I. Ho, G.B. Stringfellow, "Solid Phase Immiscibility in GaInN," *Appl. Phys. Lett.*, **69**, 1996, pp. 2701-2703.
- [13] I.H. Ho, G.B. Stringfellow, "Incomplete Solubility in Nitride Alloys," *Mater. Res. Soc. Symp. Proc.*, **449**, 1997, pp. 871-880.
- [14] A. Tabata, L.K. Teles, L.M.R. Scolfaro, J.R. Leite, A. Kharchenko, T. Frey, D.J. As, D. Schikora, K. Lischka, J. Furthmuller, F. Bechstedt, "Phase Separation Suppression in InGaN Epitaxial Layers due to Biaxial Strain," *Appl. Phys. Lett.*, **80**, 2002, pp. 769-771.
- [15] A. Zunger, "Handbook of Crystal Growth, Vol. 3", Elsevier, 1994.
- [16] T. Tanaka et al., "P-type conduction in Mg-doped GaN and $Al_{0.08}Ga_{0.92}N$ Grown by Metalorganic Vapor Phase Epitaxy," *Appl. Phys. Lett.*, **65**, 5, 1994, pp. 593-594.
- [17] W. Geerts, J.D. Mackenzie, C.R. Abernathy, S.J. Pearton, and T. Schmiedel, "Electrical Transport in p-GaN, n-InN and n-InGaN", *Solid-State Electron.*, **39**, 9, 1996, pp. 1289-1294.
- [18] O. Ambacher et al., "Two-Dimensional Electron Gases Induced by Spontaneous and Piezoelectric Polarization Charges in N- and Ga-face AlGaIn/GaN Heterostructures", *J. Appl. Phys.*, **85**, 6, 1999, pp. 3222-3233.
- [19] Z.Z. Bandic, P.M. Bridger, E.C. Piquette and T.C. McGill, "Minority Carrier Diffusion Length and Lifetime in GaN", *Appl. Phys. Lett.*, **72**, 24, 1998, pp. 3166-3168.
- [20] Y. Narukawa, S. Saijou, Y. Kawakami, S. Fujita, T. Mukai, and S. Nakamura, "Radiative and Nonradiative Recombination Processes in Ultraviolet Light-Emitting Diode Composed of an $In_{0.02}Ga_{0.98}N$ Active Layer", *Appl. Phys. Lett.*, **74**, 4, 1999, pp. 558-560.
- [21] H. Kim, D.J. Kim, S.J. Park, H. Hwang, "Effect of an Oxidized Ni/Au p Contact on the Performance of GaN/InGaN Multiple Quantum Well Light-Emitting Diodes," *J. Appl. Phys.*, **88**, 2001, pp. 1506-1508.
- [22] M. E. Lin, F. Y. Huang, and H. Morkoç, "Nonalloyed Ohmic Contacts on GaN using InN/GaN Short-Period Superlattices," *Appl. Phys. Lett.* **64**, 1997, pp. 2557.
- [23] S. Nakamura, "Growth of $In_xGa_{1-x}N$ Compound Semiconductors and High-Power InGaN/AlGaIn Double Heterostructure Violet-Light-Emitting Diodes," *Micr. J.*, **25**, 8, 1994, pp. 651-659.